arXiv:1510.03288v1 [hep-th] 12 Oct 2015

The Casimir Effect for Thick Pistons

Guglielmo Fucci*[1]

[1]*Department of Mathematics, East Carolina University, Greenville, NC 27858 USA*

(Dated: October 13, 2015)

In this work we analyze the Casimir energy and force for a *thick* piston configuration. This study is performed by utilizing the spectral zeta function regularization method. The results we obtain for the Casimir energy and force depend explicitly on the parameters that describe the general self-adjoint boundary conditions imposed. Numerical results for the Casimir force are provided for specific types of boundary conditions and are also compared to the corresponding force on an infinitely thin piston.

I. INTRODUCTION

Variations in the vacuum structure of a quantum field give rise to what is commonly know as the Casimir effect [5, 31–33]. It its simplest form it manifests itself as a net force between neutral objects [7]. Any attempt at computing the Casimir energy and force for almost all geometric configurations of neutral objects necessarily leads to divergences that need to be regularized through the use of appropriate formal methods [5]. A particular example of a configuration for which the Casimir force is, generally, well defined is provided by the so-called Casimir piston. The most general Casimir piston can be described as consisting of two compact manifolds having a common boundary which is referred to as the piston. Casimir piston configurations were first introduced in [8], and since then they have been the subject of intense research (see e.g. [2, 12–14, 24, 25, 28–30]). The main reason for such popularity lies in the fact that while the Casimir energy might present divergences, the corresponding Casimir force on the piston is well defined. It is important to point out, however, that this does not hold, in general, when the piston configuration has a non vanishing curvature [20].

Most of the research that has been performed on the Casimir effect for piston configurations has been focused almost excursively on "idealized" cases. These are cases characterized by Dirichlet, Neumann or hybrid (mixed) boundary conditions imposed at the boundary of the piston configuration, and on the piston itself. Moreover, in idealized cases, the piston is always assumed to be infinitely thin. It is not very difficult to realize that the results obtained for the Casimir energy and force in idealized cases are unsuitable for the description of piston configurations consisting of real materials for two main reasons: 1) Physical properties of real materials might not be appropriately described by any of the ideal boundary conditions (Dirichlet,

* Electronic address: fuccig@ecu.edu

Neumann or hybrid) and, 2) real materials do have a finite thickness. An attempt at addressing the first problem can be found for instance in [21] where the Casimir effect is studied for a piston configuration endowed with general boundary conditions. A different approach was undertaken in [1, 3, 17, 19] where the ideal boundary conditions were replaced by a suitable potential function which would better describe the physical properties of real materials.

The Casimir effect for materials of finite thickness, instead, has been analyzed within the framework of piston configurations for instance in [2, 36]. The main purpose of this work is to provide a more comprehensive study of the Casimir effect for piston configurations in which we consider general boundary conditions and a piston of finite thickness. It is worth noting that in this approach the boundary conditions imposed on one side of the thick piston are allowed to be independent of the boundary conditions imposed on the other side. This specific setup could be very useful in describing pistons consisting of certain anisotropic materials (those for which the anisotropy occurs along the thickness of the piston).

In this paper we will use the spectral zeta function regularization technique in order to analyze the Casimir energy and force associated with a thick piston. The spectral zeta function, $\zeta(s)$, of the problem under consideration can be used to find the Casimir energy according to the formula [5, 6, 15, 16, 27]

$$E_{\rm Cas} = \lim_{\varepsilon\to 0} \frac{\mu^{2\varepsilon}}{2}\zeta\left(\varepsilon - \frac{1}{2}\right) , \tag{1.1}$$

with μ representing a parameter with the dimensions of a mass. Due to the fact that the spectral zeta function generally develops a simple pole at the point $s = -1/2$ [27], the Casimir energy presents divergences which are easily shown in the formula

$$E_{\rm Cas} = \frac{1}{2}{\rm FP}\,\zeta\left(-\frac{1}{2}\right) + \frac{1}{2}\left(\frac{1}{\varepsilon} + \ln\mu^2\right){\rm Res}\,\zeta\left(-\frac{1}{2}\right) + O(\varepsilon) , \tag{1.2}$$

with FP and Res denoting, respectively, the finite part and the residue. It is clear, from the previous expression, that the Casimir energy becomes a well defined quantity when the residue of the spectral zeta function at $s = -1/2$ vanishes. In the case of piston configurations, the Casimir energy depends explicitly on the position of the piston a, and the corresponding Casimir force is obtained as follows

$$F_{\rm Cas}(a) = -\frac{\partial}{\partial a}E_{\rm Cas}(a) . \tag{1.3}$$

In order to get a Casimir force on the piston devoid of meaningless divergences the residue of the zeta function appearing in (1.2) has to be independent of the position of the piston a.

The outline of the paper is as follows. In the next Section we describe in details the thick piston configuration and obtain the associated spectral zeta function. In Section III we perform the analytic continuation of the spectral zeta function and obtain an explicit expression for the Casimir energy of the form indicated in

(1.2). Plots describing how the Casimir force on a thick piston varies with respect to the position of the piston itself and its thickness are provided in Section IV for several specific examples of boundary conditions. The conclusions summarize our main results and point out further directions of research.

II. SPECTRAL ZETA FUNCTION FOR THE PISTON

In order to describe the geometric configuration associated with a thick piston we consider a D-dimensional product manifold of the type $M = [0, L] \times N$ where $[0, L] \subset \mathbb{R}$ and N is a $(D-1)$-dimensional compact Riemannian manifold with or without boundary. Let a denote an arbitrary point in the interval $(0, L)$, and let $\epsilon > 0$. We then define the manifolds $N_{a-\epsilon/2}$ and $N_{a+\epsilon/2}$ to be the cross-sections of M at the point $a - \epsilon/2$ and $a + \epsilon/2$, respectively. The cross-sections constructed above naturally divide the manifold M in three regions M_I, M_{II}, and M_{III}. The regions $M_I = [0, a - \epsilon/2) \times M$ and $M_{III} = (a + \epsilon/2, L] \times M$ will be referred to as the left, respectively right, chamber of the piston configuration while the region $M_{II} = [a - \epsilon/2, a + \epsilon/2] \times M$ will describe the piston itself of thickness ϵ. It is clear that in order to have a proper piston configuration we need to assume that $\epsilon \in [0, L)$. It is not very difficult to realize that in the limit $\epsilon \to 0$ the thick piston outlined above reduces to the familiar infinitely thin Casimir piston with a general cross-section (see for instance [21]).

In this work we focus our attention on a massless scalar field confined on the piston M. The propagation of the scalar field in each region of the piston configuration is described by the following differential equation

$$\left(-\frac{\mathrm{d}^2}{\mathrm{d}x^2} - \Delta_N\right)\phi_j = \alpha_j^2 \phi_j \,, \tag{2.1}$$

with Δ_N representing the Laplace operator on the base manifold N and $j = \{I, II, III\}$. By using separation of variables the general solution to (2.1) can be written as a product $\phi_j = \varphi_j(\lambda, x)\Phi(\mathbf{x})$ where the function $\Phi(\mathbf{x})$ solves the equation $-\Delta_N \Phi(\mathbf{x}) = \lambda^2 \Phi(\mathbf{x})$ while the functions $\varphi_j(\lambda, x)$ are solutions to the second-order differential equation

$$\left(-\frac{\mathrm{d}^2}{\mathrm{d}x^2} + \lambda^2\right)\varphi_j(\lambda, x) = \alpha_j^2 \varphi_j(\lambda, x) \,. \tag{2.2}$$

The spectral zeta function needed for the analysis of the Casimir energy associated with the thick piston configuration is written as the sum

$$\zeta(s) = \zeta_I(s) + \zeta_{II}(s) + \zeta_{III}(s) \,, \tag{2.3}$$

where $\zeta_j(s)$ represents the spectral zeta function of region M_j and is defined as

$$\zeta_j(s) = \sum_{\alpha_j} \alpha_j^{-2s} \,. \tag{2.4}$$

It is well known [27], from the general theory of spectral zeta function, that $\zeta_j(s)$ in (2.4), and consequently $\zeta(s)$ in (2.3), are analytic functions in the region of the complex plane $\Re(s) > D/2$.

As we have already mentioned earlier, in order to obtain the Casimir energy for our piston configuration we need to analyze the behavior of the zeta function in the neighborhood of the point $s = -1/2$. This point, however, lies outside of the region of convergence $\Re(s) > D/2$. This last remark implies that it is necessary to perform the analytic continuation of $\zeta(s)$ to the region $\Re(s) \leq D/2$ containing $s = -1/2$. To perform the desired analytic continuation we utilize a suitable integral representation of the zeta functions $\zeta_j(s)$ [27]. A key ingredient of this representation is a function which provides an implicit equation for the eigenvalues α_j. Such function can be easily found by making use of the boundary conditions. Here we will impose, on the differential equation (2.2), general separated boundary conditions that lead to a self-adjoint boundary value problem [21, 22]. These boundary conditions are of the form [38]

$$\begin{aligned} A_1\varphi_I(\lambda,0) + A_2\varphi_I'(\lambda,0) &= 0\,, \\ B_1\varphi_I\left(\lambda, a-\frac{\epsilon}{2}\right) - B_2\varphi_I'\left(\lambda, a-\frac{\epsilon}{2}\right) &= 0\,, \end{aligned} \tag{2.5}$$

in region I,

$$\begin{aligned} B_1\varphi_{II}\left(\lambda, a-\frac{\epsilon}{2}\right) - B_2\varphi_{II}'\left(\lambda, a-\frac{\epsilon}{2}\right) &= 0\,, \\ C_1\varphi_{II}\left(\lambda, a+\frac{\epsilon}{2}\right) + C_2\varphi_{II}'\left(\lambda, a+\frac{\epsilon}{2}\right) &= 0\,, \end{aligned} \tag{2.6}$$

in region II, and

$$\begin{aligned} C_1\varphi_{III}\left(\lambda, a+\frac{\epsilon}{2}\right) + C_2\varphi_{III}'\left(\lambda, a+\frac{\epsilon}{2}\right) &= 0\,, \\ D_1\varphi_{III}(\lambda, L) - D_2\varphi_{III}'(\lambda, L) &= 0\,, \end{aligned} \tag{2.7}$$

in region III where $A_1, A_2, B_1, B_2, C_1, C_2, D_1, D_2 \in \mathbb{R}$ satisfying the conditions $(A_1, A_2) \neq (0,0)$, $(B_1, B_2) \neq (0,0)$, $(C_1, C_2) \neq (0,0)$, and $(D_1, D_2) \neq (0,0)$.

In all three regions the general solution of the differential equation (2.2) is of the form

$$\varphi_j(x) = c_j^{(+)} \exp\left\{ i\sqrt{\alpha_j^2 - \lambda^2}(x - x_j)\right\} + c_j^{(-)} \exp\left\{ -i\sqrt{\alpha_j^2 - \lambda^2}(x - x_j)\right\}\,, \tag{2.8}$$

where we have used the notation $x_I = 0$, $x_{II} = a - \epsilon/2$, and $x_{III} = a + \epsilon/2$. Now, we choose the coefficients $c_j^{(+)}$ and $c_j^{(-)}$ so that the boundary condition at the left boundary in each region is automatically satisfied. In doing so, one obtains

$$\varphi_I(\lambda,0) = -A_2 \quad , \quad \varphi_I'(\lambda,0) = A_1\,, \tag{2.9}$$

$$\varphi_{II}\left(\lambda, a-\frac{\epsilon}{2}\right) = B_2 \quad , \quad \varphi_{II}'\left(\lambda, a-\frac{\epsilon}{2}\right) = B_1\,, \tag{2.10}$$

$$\varphi_{III}\left(\lambda, a+\frac{\epsilon}{2}\right) = -C_2 \quad , \quad \varphi_{III}'\left(\lambda, a+\frac{\epsilon}{2}\right) = C_1\,. \tag{2.11}$$

The above relations allow us to rewrite the solution $\varphi_j(x)$ as

$$\varphi_j(x) = \frac{\varphi_j'(\lambda, x_j)}{\sqrt{\alpha_j^2 - \lambda^2}} \sin\left[\sqrt{\alpha_j^2 - \lambda^2}(x - x_j)\right] + \varphi_j(\lambda, x_j) \cos\left[\sqrt{\alpha_j^2 - \lambda^2}(x - x_j)\right] . \tag{2.12}$$

By imposing the remaining boundary conditions on the right boundary of each region we obtain equations that implicitly provide the eigenvalues α_j. More precisely, in region I we have

$$\begin{aligned} f_\lambda^I\left(\alpha, a - \frac{\epsilon}{2}\right) &= \left(\frac{A_1 B_1}{\sqrt{\alpha_I^2 - \lambda^2}} - A_2 B_2 \sqrt{\alpha_I^2 - \lambda^2}\right) \sin\left[\sqrt{\alpha_I^2 - \lambda^2}\left(a - \frac{\epsilon}{2}\right)\right] \\ &- (A_2 B_1 + A_1 B_2) \cos\left[\sqrt{\alpha_I^2 - \lambda^2}\left(a - \frac{\epsilon}{2}\right)\right] = 0 , \end{aligned} \tag{2.13}$$

in region II we have

$$\begin{aligned} f_\lambda^{II}(\alpha, \epsilon) &= \left(\frac{C_1 B_1}{\sqrt{\alpha_{II}^2 - \lambda^2}} - C_2 B_2 \sqrt{\alpha_{II}^2 - \lambda^2}\right) \sin\left(\sqrt{\alpha_{II}^2 - \lambda^2}\epsilon\right) \\ &+ (C_2 B_1 + C_1 B_2) \cos\left(\sqrt{\alpha_I^2 - \lambda^2}\epsilon\right) = 0 , \end{aligned} \tag{2.14}$$

and, finally, in region III we obtain

$$\begin{aligned} f_\lambda^{III}\left(\alpha, L - a - \frac{\epsilon}{2}\right) &= \left(\frac{C_1 D_1}{\sqrt{\alpha_{III}^2 - \lambda^2}} - C_2 D_2 \sqrt{\alpha_{III}^2 - \lambda^2}\right) \sin\left[\sqrt{\alpha_{III}^2 - \lambda^2}\left(L - a - \frac{\epsilon}{2}\right)\right] \\ &- (D_2 C_1 + D_1 C_2) \cos\left[\sqrt{\alpha_{III}^2 - \lambda^2}\left(L - a - \frac{\epsilon}{2}\right)\right] = 0 . \end{aligned} \tag{2.15}$$

The equations displayed above have simple zeroes which, in general, can be both real and purely imaginary [34, 35]. Since, here, we work under the assumption that all the eigenvalues α_j are positive, we will only consider instances in which all the solutions of the equations (2.13), (2.14), and (2.15) are real. These occur only for values of the parameters in the boundary conditions belonging to specific intervals of the real line (see e.g. [21]). To find these intervals it is actually more convenient to consider the equations in (2.13), (2.14), and (2.15) with the variable α_j replaced with $i\alpha_j$, namely

$$\begin{aligned} f_\lambda^I\left(i\alpha, a - \frac{\epsilon}{2}\right) &= \left(\frac{A_1 B_1}{\sqrt{\alpha_I^2 + \lambda^2}} + A_2 B_2 \sqrt{\alpha_I^2 + \lambda^2}\right) \sinh\left[\sqrt{\alpha_I^2 + \lambda^2}\left(a - \frac{\epsilon}{2}\right)\right] \\ &- (A_2 B_1 + A_1 B_2) \cosh\left[\sqrt{\alpha_I^2 + \lambda^2}\left(a - \frac{\epsilon}{2}\right)\right] = 0 , \end{aligned} \tag{2.16}$$

$$\begin{aligned} f_\lambda^{II}(i\alpha, \epsilon) &= \left(\frac{C_1 B_1}{\sqrt{\alpha_{II}^2 + \lambda^2}} + C_2 B_2 \sqrt{\alpha_{II}^2 + \lambda^2}\right) \sinh\left(\sqrt{\alpha_{II}^2 + \lambda^2}\epsilon\right) \\ &+ (C_2 B_1 + C_1 B_2) \cosh\left(\sqrt{\alpha_I^2 + \lambda^2}\epsilon\right) = 0 , \end{aligned} \tag{2.17}$$

and

$$f_{\lambda}^{III}\left(i\alpha, L-a-\frac{\epsilon}{2}\right) = \left(\frac{C_1 D_1}{\sqrt{\alpha_{III}^2+\lambda^2}} + C_2 D_2 \sqrt{\alpha_{III}^2+\lambda^2}\right)\sinh\left[\sqrt{\alpha_{III}^2+\lambda^2}\left(L-a-\frac{\epsilon}{2}\right)\right] - (D_2 C_1 + D_1 C_2)\cosh\left[\sqrt{\alpha_{III}^2+\lambda^2}\left(L-a-\frac{\epsilon}{2}\right)\right] = 0 \,. \tag{2.18}$$

Now, it is not very difficult to show that (2.16) has no real zeroes, and hence (2.13) has no purely imaginary solutions, if the following conditions are satisfied

$$\left\{\frac{A_2 B_2}{(a-\epsilon/2)^2 A_1 B_1} \leq 0 \,, \frac{1}{a-\epsilon/2}\left(\frac{A_2}{A_1}+\frac{B_2}{B_1}\right) \geq 1\right\} \,, \quad \text{or} \quad \left\{\frac{A_2}{(a-\epsilon/2)A_1} \leq 0 \,, \frac{B_2}{(a-\epsilon/2)B_1} \leq 0\right\} \,, \tag{2.19}$$

for $A_1 B_1 \neq 0$,

$$\frac{B_2}{(a-\epsilon/2)B_1} \leq 0 \,, \quad A_1 = 0 \,, \quad \text{and} \quad \frac{A_2}{(a-\epsilon/2)A_1} \leq 0 \,, \quad B_1 = 0 \,, \tag{2.20}$$

and for $A_1 = B_1 = 0$. Similar conditions apply to (2.18). In fact, (2.15) has no purely imaginary zeroes when

$$\left\{\frac{C_2 D_2}{(L-a-\epsilon/2)^2 C_1 D_1} \leq 0 \,, \frac{1}{L-a-\epsilon/2}\left(\frac{C_2}{C_1}+\frac{D_2}{D_1}\right) \geq 1\right\} \,, \quad \text{or} \quad \left\{\frac{C_2}{(L-a-\epsilon/2)C_1} \leq 0 \,, \frac{D_2}{(L-a-\epsilon/2)D_1} \leq 0\right\} \,, \tag{2.21}$$

for $C_1 D_1 \neq 0$

$$\frac{D_2}{(L-a-\epsilon/2)D_1} \leq 0 \,, \quad C_1 = 0 \,, \quad \text{and} \quad \frac{C_2}{(L-a-\epsilon/2)C_1} \leq 0 \,, \quad D_1 = 0 \,, \tag{2.22}$$

and for $C_1 = D_1 = 0$. Equation (2.14), instead, has only real solutions if

$$\left\{\frac{B_2 C_2}{\epsilon^2 B_1 C_1} \leq 0 \,, \frac{1}{\epsilon}\left(\frac{B_2}{B_1}+\frac{C_2}{C_1}\right) \leq -1\right\} \,, \quad \text{or} \quad \left\{\frac{B_2}{\epsilon B_1} \geq 0 \,, \frac{C_2}{\epsilon C_1} \geq 0\right\} \,, \tag{2.23}$$

when $B_1 C_1 \neq 0$

$$\frac{B_2}{\epsilon B_1} \geq 0 \,, \quad C_1 = 0 \,, \quad \text{and} \quad \frac{C_2}{\epsilon C_1} \geq 0 \,, \quad B_1 = 0 \,, \tag{2.24}$$

and for $C_1 = B_1 = 0$. Since, as already mentioned earlier, we are only interested in real eigenvalues α_j we assume for the rest of this work that the coefficients of the boundary conditions in (2.5), (2.6), and (2.7) satisfy the above conditions.

The equations in (2.16)-(2.18) play a fundamentally important role in expressing the spectral zeta function in each region in terms of a complex integral [27]. In our case we have

$$\zeta_j(s,\epsilon,a) = \sum_{\lambda} n(\lambda)\zeta_j^{\lambda}(s,\epsilon,a) \,, \tag{2.25}$$

where $n(\lambda)$ represents the multiplicity of the eigenvalues of the Laplacian Δ_N, and the functions $\zeta_j^\lambda(s,\epsilon,a)$ are defined as

$$\zeta_j^\lambda(s,\epsilon,a) = \frac{\sin\pi s}{\pi}\lambda^{-2s}\int_0^\infty z^{-2s}\frac{\partial}{\partial z}\ln f_\lambda^j(i\lambda z,\epsilon,a)\ , \tag{2.26}$$

with $f_\lambda^j(iz,\epsilon,a)$ given in (2.16), (2.17), and (2.18) for $j = I$, $j = II$, and $j = III$, respectively. It can be proved, by analyzing the asymptoic behavior of $f_\lambda^j(i\lambda z,\epsilon,a)$ as $z \to 0$ and as $z \to \infty$, that the integral representation (2.26) is valid in the region of the complex plane $1/2 < \Re(s) < 1$ [21].

The Casimir energy, and hence the force, is obtained from the knowledge of the spectral zeta function in the neighborhood of $s = -1/2$. Since this point does not belong to the region $1/2 < \Re(s) < 1$, the zeta function in (2.25) needs to be analytically continued to the complex semi-plane $\Re(s) \leq 1/2$.

Before concluding this Section we would like to discuss the limit of infinitely thin pistons. According to the boundary conditions (2.5)-(2.7) the left side and the right side of the thick piston are allowed to have different types of boundary conditions. However, in the limit of a thin piston, $\epsilon \to 0$, it is reasonable to assume that the boundary conditions to the left and right side of the piston must coalesce. This implies that results regarding infinitely thin pistons cannot be obtained by simply taking the limit $\epsilon \to 0$ of the ones for thick pistons. In fact the correct thin piston limit is obtained not only by performing the limit $\epsilon \to 0$ but also by imposing the following relations $B_2 = -C_2$ and $B_1 = C_1$ on the parameters describing the boundary conditions on the piston itself.

III. ANALYTIC CONTINUATION AND THE CASIMIR ENERGY

The restriction $\Re(s) > 1/2$ indicated in the previous Section is due to the behavior of the integrand in (2.26) as $\lambda z \to \infty$. In order to extend the spectral zeta function (2.25) to the region to the left of $\Re(s) = 1/2$, one needs to subtract and add an appropriate number of terms of the asymptotic expansion of $\ln f_\lambda^j(i\lambda z,\epsilon,a)$ as $\lambda \to \infty$ uniform in the variable z. To obtain the desired asymptotic expansion we use the exponential form of the hyperbolic functions to write $\ln f_\lambda^j(i\lambda z,\epsilon,a)$ in region I as

$$\begin{aligned}\ln f_\lambda^I\left(i\lambda z, a-\frac{\epsilon}{2}\right) &= \lambda\sqrt{1+z^2}\left(a-\frac{\epsilon}{2}\right) + \ln\left[\frac{A_1B_1}{2\lambda\sqrt{1+z^2}} - \frac{A_1B_2+A_2B_1}{2} + \frac{A_2B_2}{2}\lambda\sqrt{1+z^2}\right] \\ &+ \ln\left[1+\varepsilon_I(\lambda z,\epsilon,a)\right]\ ,\end{aligned} \tag{3.1}$$

in region II as

$$\begin{aligned}\ln f_\lambda^{II}(i\lambda z,\epsilon) &= \lambda\sqrt{1+z^2}\epsilon + \ln\left[\frac{B_1C_1}{2\lambda\sqrt{1+z^2}} + \frac{B_1C_2+B_2C_1}{2} + \frac{B_2C_2}{2}\lambda\sqrt{1+z^2}\right] \\ &+ \ln\left[1+\varepsilon_{II}(\lambda z,\epsilon,a)\right]\ ,\end{aligned} \tag{3.2}$$

and, finally, in region III as

$$\ln f_\lambda^{III}\left(i\lambda z, L-a-\frac{\epsilon}{2}\right) = \lambda\sqrt{1+z^2}\left(L-a-\frac{\epsilon}{2}\right)+\ln\left[\frac{C_1D_1}{2\lambda\sqrt{1+z^2}}-\frac{C_1D_2+C_2D_1}{2}+\frac{C_2D_2}{2}\lambda\sqrt{1+z^2}\right] + \ln\left[1+\varepsilon_{III}(\lambda z,\epsilon,a)\right] , \tag{3.3}$$

where the functions $\varepsilon_j(\lambda z,\epsilon,a)$ describe the exponentially small terms. The specific form of the uniform asymptotic expansion depends on the value of some of the parameters in the boundary conditions (2.5)-(2.7) [22]. For instance, the asymptotic expansion for $\ln f_\lambda^I(i\lambda z, a-\epsilon/2)$ as $\lambda\to\infty$ uniform in z depends on whether the coefficients A_2, B_2 or both are either zero or different than zero. The possible combinations lead to four different forms of the uniform asymptotic expansion of $\ln f_\lambda^I(i\lambda z, a-\epsilon/2)$. Obviously, the same remarks hold true for $\ln f_\lambda^{II}(i\lambda z,\epsilon)$ with the parameters B_2 and C_2, and for $\ln f_\lambda^{III}(i\lambda z, L-a-\epsilon/2)$ with the parameters C_2 and D_2.

A detailed description on how to obtain the uniform asymptotic expansion of $\ln f_\lambda^j(i\lambda z,\epsilon,a)$ can be found in [21] and, for the sake of brevity, will not be repeated here. We focus, instead, on the final results. By introducing the function

$$\delta(x)=\begin{cases}1 & \text{if } x=0\\ 0 & \text{if } x\neq 0\end{cases} , \tag{3.4}$$

we can write the different forms of the uniform asymptotic expansion in one expression. In particular, one obtains, in region I,

$$\begin{aligned}\ln f_\lambda^I\left(i\lambda z, a-\frac{\epsilon}{2}\right) \sim\ & \lambda\sqrt{1+z^2}\left(a-\frac{\epsilon}{2}\right)+[1-\delta(A_2B_2)-\delta(A_2)\delta(B_2)]\ln\left(\lambda\sqrt{1+z^2}\right)\\ &+[1-\delta(A_2B_2)]\ln\left(\frac{A_2B_2}{2}\right)+\delta(A_2)\delta(B_2)\ln\left(\frac{A_1B_1}{2}\right)\\ &+[\delta(A_2B_2)-\delta(A_2)\delta(B_2)]\ln\left(-\frac{A_1B_2\delta(A_2)+A_2B_1\delta(B_2)}{2}\right)+\sum_{k=1}^{\infty}\frac{g_k^I}{\lambda^k(1+z^2)^{\frac{k}{2}}} ,\end{aligned} \tag{3.5}$$

where

$$g_k^I=\left(\frac{\delta(A_2B_2)-1}{k}\right)\left[\left(\frac{A_1}{A_2}\right)^k+\left(\frac{B_1}{B_2}\right)^k\right]+\left(\frac{\delta(A_2B_2)-\delta(A_2)\delta(B_2)}{k}\right)\left(\frac{A_1B_1}{A_1B_2\delta(A_2)+A_2B_1\delta(B_2)}\right)^k , \tag{3.6}$$

in region II,

$$\begin{aligned}\ln f_\lambda^{II}(i\lambda z,\epsilon) \sim\ & \lambda\sqrt{1+z^2}\epsilon+[1-\delta(B_2C_2)-\delta(B_2)\delta(C_2)]\ln\left(\lambda\sqrt{1+z^2}\right)+[1-\delta(B_2C_2)]\ln\left(\frac{B_2C_2}{2}\right)\\ &+\delta(B_2)\delta(C_2)\ln\left(\frac{B_1C_1}{2}\right)+[\delta(B_2C_2)-\delta(B_2)\delta(C_2)]\ln\left(\frac{B_1C_2\delta(B_2)+B_2C_1\delta(C_2)}{2}\right)\\ &+\sum_{k=1}^{\infty}\frac{(-1)^kg_k^{II}}{\lambda^k(1+z^2)^{\frac{k}{2}}} ,\end{aligned} \tag{3.7}$$

with

$$g_k^{II} = \left(\frac{\delta(B_2C_2)-1}{k}\right)\left[\left(\frac{B_1}{B_2}\right)^k + \left(\frac{C_1}{C_2}\right)^k\right] + \left(\frac{\delta(B_2C_2)-\delta(B_2)\delta(C_2)}{k}\right)\left(\frac{B_1C_1}{B_1C_2\delta(B_2)+B_2C_1\delta(C_2)}\right)^k , \quad (3.8)$$

and in region III

$$\begin{aligned}\ln f_\lambda^{III}\left(i\lambda z, L-a-\frac{\epsilon}{2}\right) \sim\ & \lambda\sqrt{1+z^2}\left(L-a-\frac{\epsilon}{2}\right) + [1-\delta(C_2D_2)-\delta(C_2)\delta(D_2)]\ln\left(\lambda\sqrt{1+z^2}\right)\\ &+ [1-\delta(C_2D_2)]\ln\left(\frac{C_2D_2}{2}\right) + \delta(C_2)\delta(D_2)\ln\left(\frac{C_1D_1}{2}\right)\\ &+ [\delta(C_2D_2)-\delta(C_2)\delta(D_2)]\ln\left(-\frac{C_1D_2\delta(C_2)+C_2D_1\delta(D_2)}{2}\right)\\ &+ \sum_{k=1}^{\infty}\frac{g_k^{III}}{\lambda^k(1+z^2)^{\frac{k}{2}}} , \end{aligned} \quad (3.9)$$

where

$$g_k^{III} = \left(\frac{\delta(C_2D_2)-1}{k}\right)\left[\left(\frac{C_1}{C_2}\right)^k + \left(\frac{D_1}{D_2}\right)^k\right] + \left(\frac{\delta(C_2D_2)-\delta(C_2)\delta(D_2)}{k}\right)\left(\frac{C_1D_1}{C_1D_2\delta(C_2)+C_2D_1\delta(D_2)}\right)^k . \quad (3.10)$$

The explicit knowledge of the uniform asymptotic expansions (3.5), (3.7), and (3.9) allows us to proceed with the analytic continuation of the spectral zeta function $\zeta_j(s,\epsilon,a)$ in (2.25). By subtracting and adding, in the integral (2.26) representing $\zeta_j^\lambda(s,\epsilon,a)$, N terms of the expansion for $\ln f_\lambda^j(i\lambda z,\epsilon,a)$ we obtain the analytically continued expression for the spectral zeta function in (2.25) of the form

$$\zeta_j(s,\epsilon,a) = Z_j(s,\epsilon,a) + \sum_{i=-1}^{N} R_i^j(s,\epsilon,a) . \quad (3.11)$$

By construction, the function $Z_j(s,\epsilon,a)$ is analytic in the semi-plane $\Re(s) > (d-N-1)/2$ and $R_i^j(s,\epsilon,a)$ is a meromorphic function of $s\in\mathbb{C}$. Clearly, their specific expression depends on the region j. By introducing the spectral zeta function associated with the Laplacian on the manifold N

$$\zeta_N(s) = \sum_\lambda n(\lambda)\lambda^{-2s} , \quad (3.12)$$

in region I we have

$$\begin{aligned} Z_I(s,\epsilon,a) =\ & \frac{\sin\pi s}{\pi}\sum_\lambda n(\lambda)\lambda^{-2s}\int_0^\infty z^{-2s}\left[\frac{\partial}{\partial z}\ln f_\lambda^I\left(i\lambda z, a-\frac{\epsilon}{2}\right) - \lambda\sqrt{1+z^2}\left(a-\frac{\epsilon}{2}\right)\right.\\ &- [1-\delta(A_2B_2)]\ln\left(\frac{A_2B_2}{2}\right) - [1-\delta(A_2B_2)-\delta(A_2)\delta(B_2)]\ln\left(\lambda\sqrt{1+z^2}\right)\\ &- \delta(A_2)\delta(B_2)\ln\left(\frac{A_1B_1}{2}\right) - [\delta(A_2B_2)-\delta(A_2)\delta(B_2)]\ln\left(-\frac{A_1B_2\delta(A_2)+A_2B_1\delta(B_2)}{2}\right)\\ &\left.- \sum_{k=1}^{N}\frac{g_k^I}{\lambda^k(1+z^2)^{\frac{k}{2}}}\right]\mathrm{d}z , \end{aligned} \quad (3.13)$$

with

$$R^I_{-1}(s,\epsilon,a) = \frac{a-\epsilon/2}{2\sqrt{\pi}\Gamma(s)}\Gamma\left(s-\frac{1}{2}\right)\zeta_N\left(s-\frac{1}{2}\right)\,, \quad R^I_0(s,\epsilon,a) = \frac{1}{2}\left[1-\delta(A_2B_2)-\delta(A_2)\delta(B_2)\right]\zeta_N(s)\,, \tag{3.14}$$

and, for $i \geq 1$,

$$R^I_i(s,\epsilon,a) = -\frac{g^I_i}{\Gamma\left(\frac{i}{2}\right)\Gamma(s)}\Gamma\left(s+\frac{i}{2}\right)\zeta_N\left(s+\frac{i}{2}\right)\,. \tag{3.15}$$

In region II we find, instead,

$$\begin{aligned} Z_{II}(s,\epsilon) \;=\; & \frac{\sin\pi s}{\pi}\sum_\lambda n(\lambda)\lambda^{-2s}\int_0^\infty z^{-2s}\Bigg[\frac{\partial}{\partial z}\ln f^{II}_\lambda(i\lambda z,\epsilon) - \lambda\sqrt{1+z^2}\epsilon - \left[1-\delta(B_2C_2)\right]\ln\left(\frac{B_2C_2}{2}\right) \\ & - \left[1-\delta(B_2C_2)-\delta(B_2)\delta(C_2)\right]\ln\left(\lambda\sqrt{1+z^2}\right) - \delta(B_2)\delta(C_2)\ln\left(\frac{B_1C_1}{2}\right) \\ & - \left[\delta(B_2C_2)-\delta(B_2)\delta(C_2)\right]\ln\left(\frac{B_1C_2\delta(B_2)+B_2C_1\delta(C_2)}{2}\right) - \sum_{k=1}^N\frac{(-1)^k g^{II}_k}{\lambda^k(1+z^2)^{\frac{k}{2}}}\Bigg]\mathrm{d}z\,, \end{aligned} \tag{3.16}$$

where

$$R^{II}_{-1}(s,\epsilon,a) = \frac{\epsilon}{2\sqrt{\pi}\Gamma(s)}\Gamma\left(s-\frac{1}{2}\right)\zeta_N\left(s-\frac{1}{2}\right)\,, \quad R^{II}_0(s,\epsilon,a) = \frac{1}{2}\left[1-\delta(B_2C_2)-\delta(B_2)\delta(C_2)\right]\zeta_N(s)\,, \tag{3.17}$$

and

$$R^{II}_i(s,\epsilon,a) = \frac{(-1)^{i+1}g^{II}_i}{\Gamma\left(\frac{i}{2}\right)\Gamma(s)}\Gamma\left(s+\frac{i}{2}\right)\zeta_N\left(s+\frac{i}{2}\right)\,, \tag{3.18}$$

for for $i \geq 1$. Finally, in region III we get

$$\begin{aligned} Z_{III}(s,\epsilon,a) \;=\; & \frac{\sin\pi s}{\pi}\sum_\lambda n(\lambda)\lambda^{-2s}\int_0^\infty z^{-2s}\Bigg[\frac{\partial}{\partial z}\ln f^{III}_\lambda\left(i\lambda z, L-a-\frac{\epsilon}{2}\right) - \lambda\sqrt{1+z^2}\left(L-a-\frac{\epsilon}{2}\right) \\ & - \left[1-\delta(C_2D_2)\right]\ln\left(\frac{C_2D_2}{2}\right) - \left[1-\delta(C_2D_2)-\delta(C_2)\delta(D_2)\right]\ln\left(\lambda\sqrt{1+z^2}\right) \\ & - \delta(C_2)\delta(D_2)\ln\left(\frac{C_1D_1}{2}\right) - \left[\delta(C_2D_2)-\delta(C_2)\delta(D_2)\right]\ln\left(-\frac{C_1D_2\delta(C_2)+C_2D_1\delta(D_2)}{2}\right) \\ & - \sum_{k=1}^N\frac{g^{III}_k}{\lambda^k(1+z^2)^{\frac{k}{2}}}\Bigg]\mathrm{d}z\,, \end{aligned} \tag{3.19}$$

with

$$R^{III}_{-1}(s,\epsilon,a) = \frac{L-a-\epsilon/2}{2\sqrt{\pi}\Gamma(s)}\Gamma\left(s-\frac{1}{2}\right)\zeta_N\left(s-\frac{1}{2}\right)\,, \quad R^{III}_0(s,\epsilon,a) = \frac{1}{2}\left[1-\delta(C_2D_2)-\delta(C_2)\delta(D_2)\right]\zeta_N(s)\,, \tag{3.20}$$

and, for $i \geq 1$,

$$R^{III}_i(s,\epsilon,a) = -\frac{g^{III}_i}{\Gamma\left(\frac{i}{2}\right)\Gamma(s)}\Gamma\left(s+\frac{i}{2}\right)\zeta_N\left(s+\frac{i}{2}\right)\,. \tag{3.21}$$

It is important to make a remark at this point. In performing the analytic continuation of the spectral zeta function we have assumed, without explicitly mentioning it, that the Laplacian on manifold N possesses no zero modes. If a zero mode is present, then the process of analytic continuation has to be modified. This is due to the fact that the asymptotic expansions utilized above become somewhat different when dealing with zero modes. The interested reader can find the details of this case reported in [21].

By setting $N = D$ in (3.11) and by using (2.3) we obtain an expression for the spectral zeta function associated with the thick piston valid in the region $-1 < \Re(s) < 1$ and, hence, suitable for the analysis of the Casimir energy. In more details we have

$$\begin{aligned}\zeta(s,\epsilon,a) &= Z_I(s,\epsilon,a) + Z_{II}(s,\epsilon) + Z_{III}(s,\epsilon,a) + \frac{L}{2\sqrt{\pi}\Gamma(s)}\Gamma\left(s-\frac{1}{2}\right)\zeta_N\left(s-\frac{1}{2}\right)\\ &+ \frac{1}{2}\left[3-\delta(A_2B_2)-\delta(B_2C_2)-\delta(C_2D_2)-\delta(A_2)\delta(B_2)-\delta(B_2)\delta(C_2)-\delta(C_2)\delta(D_2)\right]\zeta_N(s)\\ &- \sum_{i=1}^{D}\frac{g_i^I+(-1)^i g_i^{II}+g_i^{III}}{\Gamma\left(\frac{i}{2}\right)\Gamma(s)}\Gamma\left(s+\frac{i}{2}\right)\zeta_N\left(s+\frac{i}{2}\right)\,. \end{aligned} \tag{3.22}$$

The Casimir energy is obtained from this expression by first setting $s = \omega - 1/2$ and by then performing the asymptotic expansion as $\omega \to 0$. To complete this task special attention needs to be paid to the meromorphic structure of $\zeta_N(s)$ which, according to the theory of spectral zeta functions [23, 27], reads

$$\zeta_N(\omega-n) = \frac{(-1)^n n!}{(4\pi)^{\frac{d}{2}}}A^N_{\frac{d}{2}+n} + \omega\zeta'_N(-n) + O(\omega^2)\,, \tag{3.23}$$

$$\zeta_N\left(\omega+\frac{d-k}{2}\right) = \frac{A^N_{k/2}}{\omega\Gamma\left(\frac{d-k}{2}\right)} + \mathrm{FP}\,\zeta_N\left(\frac{d-k}{2}\right) + O(\omega)\,, \tag{3.24}$$

$$\zeta_N\left(\omega-\frac{2n+1}{2}\right) = \frac{A^N_{(d+2n+1)/2}}{\omega\Gamma\left(-\frac{2n+1}{2}\right)} + \mathrm{FP}\,\zeta_N\left(-\frac{2n+1}{2}\right) + O(\omega)\,, \tag{3.25}$$

where $n \in \mathbb{N}_0$, $k = \{0,\ldots,d-1\}$, and $A^N_{m/2}$ are the coefficients of the small-t asymptotic expansion of the trace of the heat kernel associated with the Laplacian Δ_N [23, 37].

By using the formula (3.22) and the pole structure displayed in (3.23)-(3.25) we obtain for the Casimir

energy of the thick piston the following expression

$$
\begin{aligned}
E_{\rm Cas}(\epsilon,a) = \frac{1}{2}\left(\frac{1}{\omega}+\ln\mu^2\right)\Bigg\{ & -\frac{1}{4\sqrt{\pi}}[3-\delta(A_2B_2)-\delta(B_2C_2)-\delta(C_2D_2)-\delta(A_2)\delta(B_2)-\delta(B_2)\delta(C_2) \\
& -\delta(C_2)\delta(D_2)]A^N_{\frac{d+1}{2}} - \frac{L}{(4\pi)^{\frac{d+2}{2}}}A^N_{\frac{d+2}{2}} + 2\frac{g_1^I-g_1^{II}+g_1^{III}}{(4\pi)^{\frac{d+2}{2}}}A^N_{\frac{d}{2}} + \sum_{k=2}^{D}\frac{g_k^I+(-1)^k g_k^{II}+g_k^{III}}{2\sqrt{\pi}\Gamma\left(\frac{k}{2}\right)}A^N_{\frac{d+1-k}{2}}\Bigg\} \\
& + \frac{1}{2}Z_I\left(-\frac{1}{2},\epsilon,a\right)+\frac{1}{2}Z_{II}\left(-\frac{1}{2},\epsilon\right)+\frac{1}{2}Z_{III}\left(-\frac{1}{2},\epsilon,a\right)+\frac{L}{8\pi}\left[\zeta'_N(-1)-\frac{2\ln 2-1}{(4\pi)^{\frac{d}{2}}}A^N_{\frac{d+2}{2}}\right] \\
& + \frac{1}{4}\left[3-\delta(A_2B_2)-\delta(B_2C_2)-\delta(C_2D_2)-\delta(A_2)\delta(B_2)-\delta(B_2)\delta(C_2)-\delta(C_2)\delta(D_2)\right]\mathrm{FP}\,\zeta_N\left(-\frac{1}{2}\right) \\
& + \frac{g_1^I-g_1^{II}+g_1^{III}}{4\pi}\left[\zeta'_N(0)+\frac{2(\ln 2-1)}{(4\pi)^{\frac{d}{2}}}A^N_{\frac{d}{2}}\right] \\
& + \sum_{k=2}^{D}\frac{g_k^I+(-1)^k g_k^{II}+g_k^{III}}{4\sqrt{\pi}\Gamma\left(\frac{k}{2}\right)}\left[\Gamma\left(\frac{k-1}{2}\right)\mathrm{FP}\,\zeta_N\left(\frac{k-1}{2}\right)+\left(2-\gamma-2\ln 2+\Psi\left(\frac{k-1}{2}\right)\right)A^N_{\frac{d+1-k}{2}}\right]+O(\omega)\,.
\end{aligned}
\tag{3.26}
$$

It is well-known that the Casimir energy of a piston is generally not a well defined quantity. This feature can clearly be seen from the above expression: In fact, the ambiguity in the Casimir energy is explicitly dependent on the heat kernel coefficients $A^N_{(d+1-k)/2}$ with $k=\{-2,\ldots,d+1\}$ and, consequently, on the geometry of the manifold N.

IV. THE CASIMIR FORCE ON PARTICULAR THICK PISTONS

Although for a general piston configuration the Casimir energy is not well defined, the Casimir force on the piston itself can be proved to be unambiguous. From the definition of the Casimir force in (1.3), it is not very difficult to obtain, from (3.26),

$$
F_{\rm Cas}(\epsilon,a) = -\frac{1}{2}Z'_I\left(-\frac{1}{2},\epsilon,a\right)-\frac{1}{2}Z'_{III}\left(-\frac{1}{2},\epsilon,a\right)\,, \tag{4.1}
$$

where the prime denotes differentiation with respect to the position of the piston a. We would like to point out that since the function Z_{II} is independent of the parameter a, there is no contribution, as one would expect, to the Casimir force on the thick piston coming from region II (namely the piston itself). The formulas obtained in (3.26) for the Casimir energy and in (4.1) for the corresponding force on the piston are valid for any smooth, compact Riemannian manifold N and for separated boundary conditions satisfying the constraints (2.19) through (2.24). In order to study more explicit examples of Casimir force on the thick piston we need to specify the manifold N. In this Section we assume that the cross-section N of the piston configuration is a d-dimensional sphere. In this circumstance the eigenvalues λ associated with the

Laplacian on N are known to be

$$\lambda = l - \frac{d-1}{2} \ , \tag{4.2}$$

with $\in \mathbb{N}_0$. It can also be shown that each eigenvalue in (4.2) has multiplicity

$$n(l) = (2l + d - 1)\frac{(l + d - 2)!}{l!(d-1)!} \ . \tag{4.3}$$

We can now use the specific formulas (4.2) and (4.3) in (4.1) and analyze how the Casimir force on a thick piston with spherical cross-section behaves as the boundary conditions change within the constraints (2.19)-(2.24). Due to the form of $Z_j\,(s, \epsilon, a)$ it is clear that that the Casimir force has to be studied numerically. At this point, however, it is important to make a remark. From the expressions (3.13), (3.22), and (4.1) it is apparent that functions Z_I, Z_{II}, and Z_{III}, and consequantly the Casimir force in (4.1), depend explicitly not only on the position of the piston a and its thickness ϵ, but also on the parameters describing the boundary conditions in (2.5), (2.6), and (2.7). Any attempt at a numerical study of the behavior of the Casimir force on a thick piston as all the parameters vary simultaneously would lead to quite complex results that would not show the role that each parameter plays in the Casimir force. For this reason, in order simplify the analysis, we fix some of the parameters and let the remaining ones be free to vary according to the constraints (2.19)-(2.24). In what follows we will work under the assumption that the manifold N is of dimension $d = 2$, and without loss of generality, we will consider a piston configuration of unit length $L = 1$.

The graphs we provide next in this Section display the Casimir force on the thick piston as a function of the position a in a number of particular cases. The lines of different thickness in each graph provide a plot of the Casimir force on pistons of varying thickness: thicker lines represent the force on thicker pistons. In all the examples outlined in this Section, we have considered the following values: $\epsilon = 0.01$, $\epsilon = 0.05$, $\epsilon = 0.2$, and $\epsilon = 0.5$. For each example considered we also examine the limit of infinitely thin pistons $\epsilon \to 0$. The infinitely thin piston case has been analyzed in details in [21] and the results found there have been used to obtain the plots, displayed with dashed lines, of the Casimir force as a function of the position of the piston a.

A. Dirichlet Boundary Conditions

As a first example we consider the case in which Dirichlet boundary conditions are imposed on the left-end of the piston configuration, that is at $x = 0$. On the left edge of the thick piston we impose general boundary conditions described by a parameter α while on its right edge and on the right-end of the piston

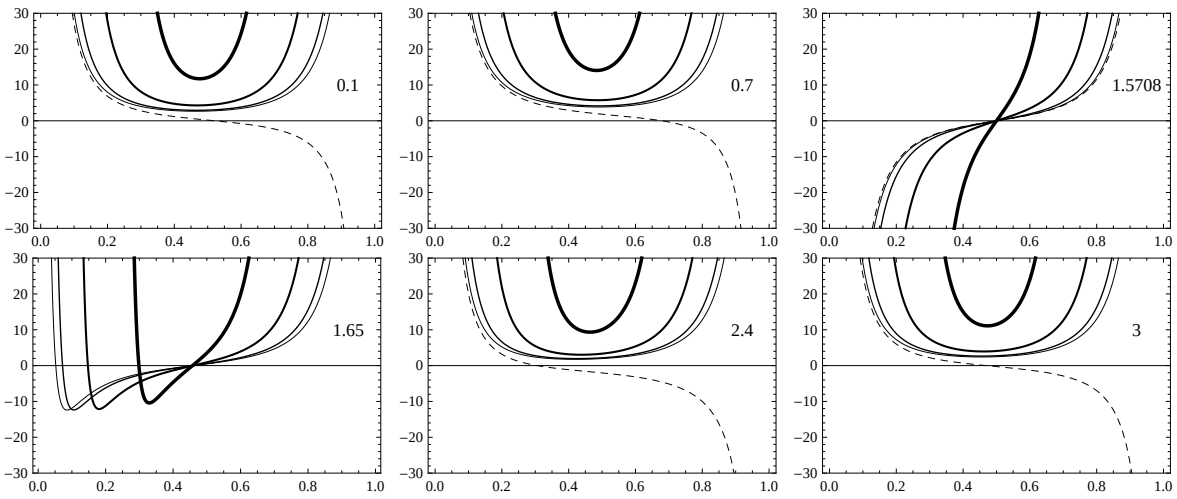

Figure 1: Dirichlet boundary conditions at the endpoints: DGDD case. Each graph is obtained by fixing the value of the parameter α, displayed in the upper right corner, in the intervals $[0, \pi/4]$ and $[\pi/2, \pi]$. The parameter a varies along the x-axis, while the Casimir force on the piston (in units for which $h = c = 1$) varies along the y-axis.

configuration we have Dirichlet boundary conditions. This set-up, which we will refer to as DGDD, is expressed in terms of the parameters in the boundary conditions (2.5)-(2.7) as follows

$$A_1 = 1\ , A_2 = 0\ , B_1 = \sin\alpha\ , B_2 = \cos\alpha\ , C_1 = 1\ , C_2 = 0\ , D_1 = 1\ , D_2 = 0\ . \tag{4.4}$$

In this, as well as in the ensuing examples, we assume, without loss of generality, that $\alpha \in [0, \pi]$. In region I the conditions (2.19) provide the following relations for the parameter α

$$\frac{\cot\alpha}{a - \epsilon/2} \geq 1\ , \quad \text{or} \quad \cot\alpha \leq 0\ . \tag{4.5}$$

These inequalities are satisfied uniformly in a and ϵ if $\alpha \in [0, \pi/4]$ or $\alpha \in [\pi/2, \pi]$. The Casimir force on a thick piston for this configuration is given in Figure 1. For infinitely thin pistons the parameter α can take values in the intervals $[0, \pi/4]$, $[3\pi/4, \pi]$ and take the value $\alpha = \pi/2$ [21]. This remark implies, in particular, that while the Casimir force on thick pistons is well defined for $\alpha \in (\pi/4, \pi/2)$ and $\alpha \in (\pi/2, 3\pi/4)$, the corresponding force on infinitely thin pistons is not. This is the reason why the dashed line is not present in one of the graphs in Figure 1.

In the next example, we consider Dirichlet boundary conditions at both endpoints of the piston configuration $x = 0$ and $x = 1$. On the left edge of the thick piston we impose general boundary conditions, parametrized by α, and on the right of the piston we consider Neumann boundary conditions. For brevity, we refer to this configuration as DGND and it is described, in terms of the parameters in the boundary conditions (2.5)-(2.7), as

$$A_1 = 1\ , A_2 = 0\ , B_1 = \sin\alpha\ , B_2 = \cos\alpha\ , C_1 = 0\ , C_2 = 1\ , D_1 = 1\ , D_2 = 0\ . \tag{4.6}$$

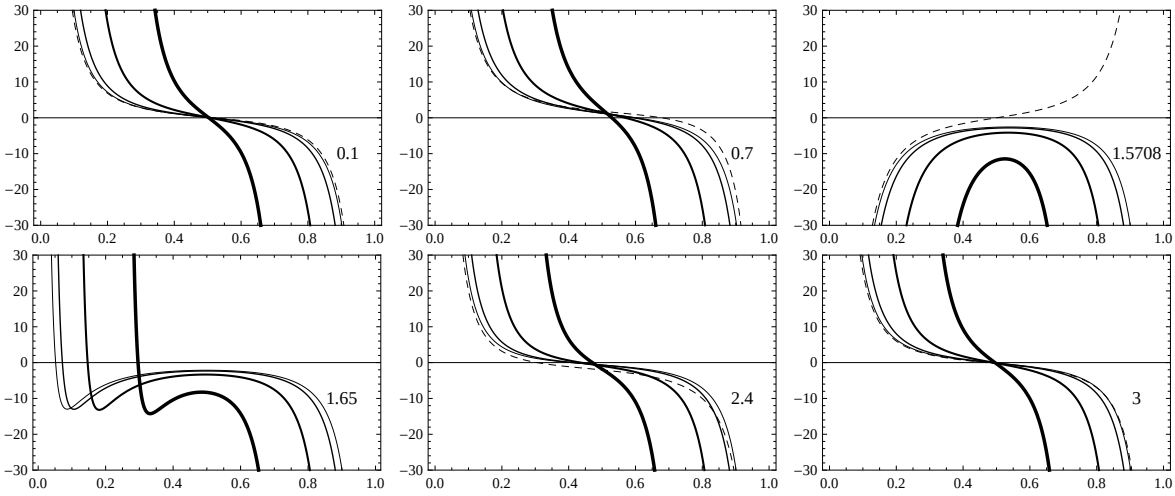

Figure 2: Dirichlet boundary conditions at the endpoints: DGND case. Each graph is obtained by fixing the value of the parameter α, displayed in the lower right corner, in the intervals $[0, \pi/4]$ and $[\pi/2, \pi]$. The parameter a varies along the x-axis, while the Casimir force on the piston (in units for which $h = c = 1$) varies along the y-axis.

According to the constraints (2.19) the parameter α has to satisfy the inequalities (4.5) which hold uniformly in a and ϵ if, once again, $\alpha \in [0, \pi/4]$ or $\alpha \in [\pi/2, \pi]$. The Casimir force on a tick piston for this case is displayed in Figure 2. The Casimir force on the corresponding infinitely thin piston, represented by the dashed lines in Figure 2, is the same as the one obtained in the DGDD case.

B. Neumann Boundary Conditions

Here we analyze the case of Neumann boundary conditions at both endpoints of the piston configuration, namely at $x = 0$ and $x = 1$. On the left side of the thick piston we have general boundary conditions, described by the parameter α, and on the right side of the piston we impose Neumann boundary condition. This configuration will be referred to as NGNN and is obtained from the conditions in (2.5)-(2.7) by setting

$$A_1 = 0 \, , A_2 = 1 \, , B_1 = \sin\alpha \, , B_2 = \cos\alpha \, , C_1 = 0 \, , C_2 = 1 \, , D_1 = 0 \, , D_2 = 1 \, . \tag{4.7}$$

The relations found in (2.20) lead to the following inequality

$$\frac{\cot\alpha}{a - \epsilon/2} \leq 0 \, , \tag{4.8}$$

which is satisfied for values of α in the interval $\alpha \in [\pi/2, \pi]$, and for $\alpha = 0$. The Casimir force on a thick piston for this particular case is shown in Figure 3. The Casimir force on the corresponding infinitely thin piston is well defined for the values $\alpha = 0$ and $\alpha = \pi/2$ [21] and is displayed via dashed lines in Figure 3.

As a further example, we consider Neumann boundary conditions at the endpoints $x = 0$ and $x = 1$, general boundary conditions on the left side of the thick piston and Dirichlet boundary conditions on its

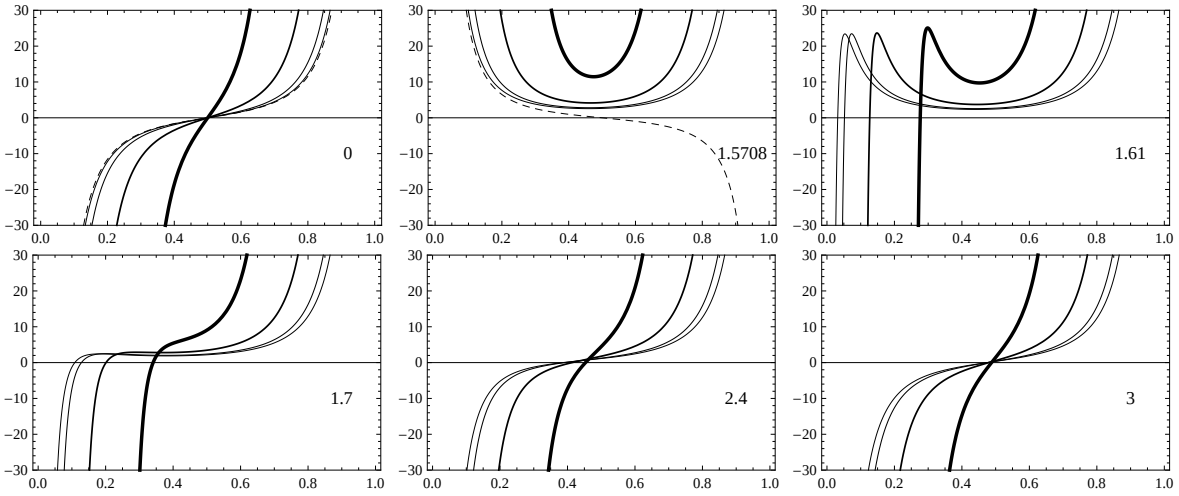

Figure 3: Neumann boundary conditions at both endpoints: NGNN case. Each graph is obtained by fixing the value of the parameter α, displayed in the lower right corner, in the interval $[\pi/2, \pi]$ and for $\alpha = 0$. The parameter a varies along the x-axis, while the Casimir force on the piston (in units for which $h = c = 1$) varies along the y-axis.

right side. This configuration, which we denote by NGDN, is obtained by using the following values for the parameters in the boundary conditions (2.5)-(2.7)

$$A_1 = 0\ , A_2 = 1\ , B_1 = \sin\alpha\ , B_2 = \cos\alpha\ , C_1 = 1\ , C_2 = 0\ , D_1 = 0\ , D_2 = 1\ . \tag{4.9}$$

Also in this example the parameter α must satisfy the inequality (4.8) which implies that $\alpha \in [\pi/2, \pi]$ and $\alpha = 0$. The Casimir force on a thick piston for this case is given in Figure 4. Furthermore, we point out that the Casimir force on the corresponding infinitely thin piston, illustrated by the dashed lines in Figure 3, is the same as the one obtained in the NGNN case.

C. Hybrid Boundary Conditions

We consider now mixed boundary conditions. On the left end of the piston configuration we impose Dirichlet boundary conditions while on the right end we impose Neuman boundary conditions. On the left side of the thick piston we have general boundary conditions, parametrized by α, and on the right side of the piston we have Dirichlet boundary conditions. This particular example will be denoted by DGDN and is obtained by setting in (2.5)-(2.7)

$$A_1 = 1\ , A_2 = 0\ , B_1 = \sin\alpha\ , B_2 = \cos\alpha\ , C_1 = 1\ , C_2 = 0\ , D_1 = 0\ , D_2 = 1\ . \tag{4.10}$$

In this case the parameter α has to satisfy the inequality (4.5) which occurs when $\alpha \in [0, \pi/4]$ or $\alpha \in [\pi/2, \pi]$. Graphs of the Casimir force on a thick piston for this example are provided in Figure 5. The corresponding

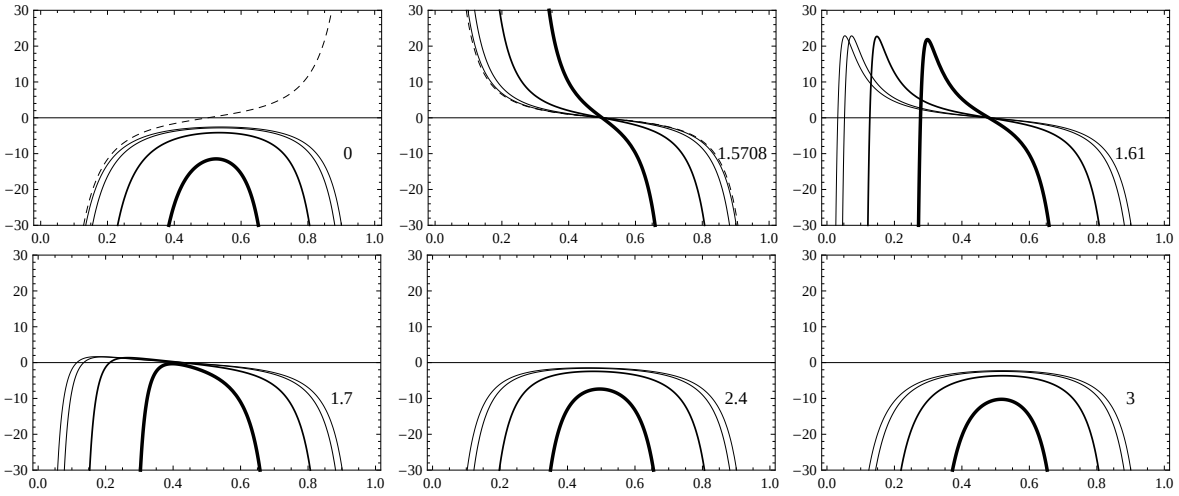

Figure 4: Neumann boundary conditions at both endpoints: NGDN case. Each graph is obtained by fixing the value of the parameter α, displayed in the lower right corner, in the interval $[\pi/2, \pi]$ and for $\alpha = 0$. The parameter a varies along the x-axis, while the Casimir force on the piston (in units for which $h = c = 1$) varies along the y-axis.

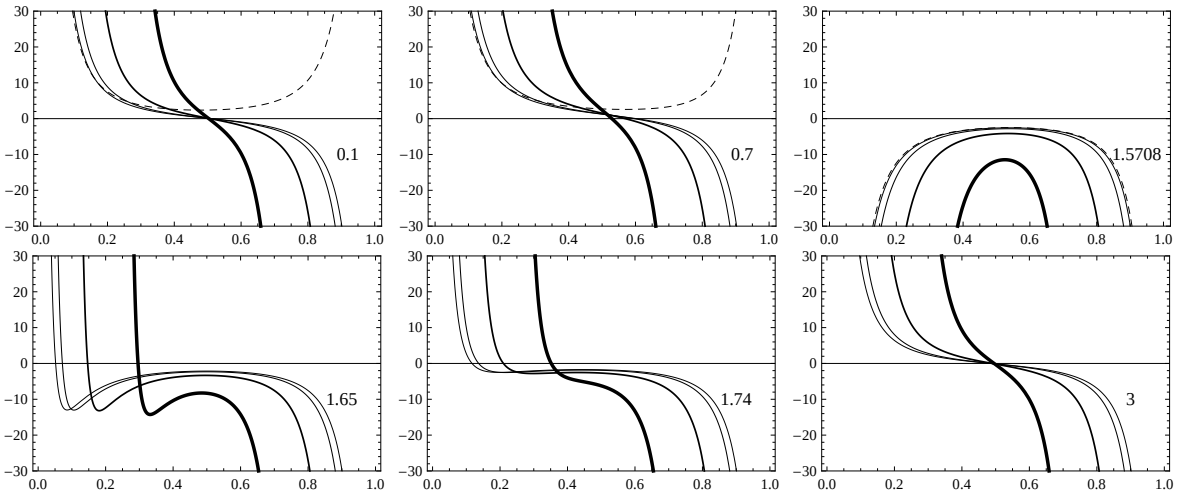

Figure 5: Hybrid boundary conditions: DGDN case. Each graph is obtained by fixing the value of the parameter α, displayed in the lower right corner, in the intervals $[0, \pi/4]$ and $[\pi/2, \pi]$. The parameter a varies along the x-axis, while the Casimir force on the piston (in units for which $h = c = 1$) varies along the y-axis.

Casimir force on the infinitely thin piston is well defined for $\alpha \in [0, \pi/4]$ and for $\alpha = \pi/2$ [21], and, once again, is displayed in Figure 5 using dashed lines.

As a last example we consider Dirichlet boundary conditions on the left end of the piston configuration and Neumann boundary condition on the right end. To the left side of the thick piston we impose general boundary conditions and on the right side of the piston we impose Neumann boundary conditions. This

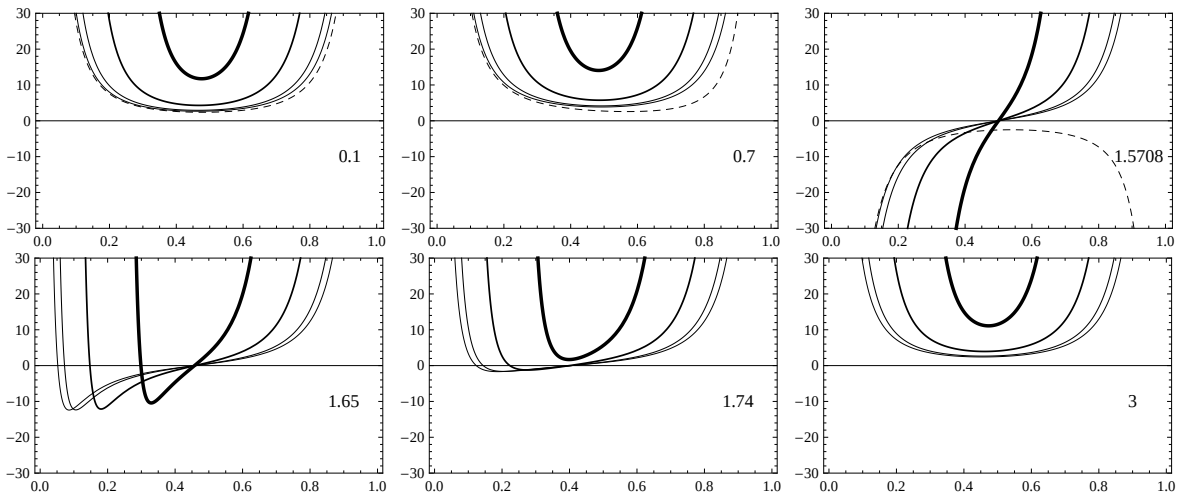

Figure 6: Hybrid boundary conditions: DGNN case. Each graph is obtained by fixing the value of the parameter α, displayed in the lower right corner, in the intervals $[0, \pi/4]$ and $[\pi/2, \pi]$. The parameter a varies along the x-axis, while the Casimir force on the piston (in units for which $h = c = 1$) varies along the y-axis.

configuration, which we name DGNN, is obtained from (2.5)-(2.7) by using the values

$$A_1 = 1\ , A_2 = 0\ , B_1 = \sin\alpha\ , B_2 = \cos\alpha\ , C_1 = 0\ , C_2 = 1\ , D_1 = 0\ , D_2 = 1\ . \tag{4.11}$$

Also in this case the parameter α is constrained to belong in the intervals $[0, \pi/4]$ or $[\pi/2, \pi]$ and plots of the Casimir force on a thick piston are provided in Figure 6. The Casimir force in the limit of infinitely thin piston for this particular example is the same as the one obtained in the DGDN case and is represented by the dashed lines.

It is worth, at this point, to briefly comment on the results obtained in this Section for the Casimir force.

In every example considered here one can notice that the Casimir force acting on the piston increases in absolute value as the thickness of the piston increases. In other words, the finite thickness somewhat "amplifies" the Casimir force acting on the piston. There are a few cases in which the Casimir force vanishes at more than one point in the interval $[0, 1]$, a behavior that has been already observed for infinitely thin pistons with general boundary conditions [21]. It is interesting to notice that the position of one of the two equilibrium points varies as the thickness of the piston changes. In all of the examples provided above, there are specific values (or a range of values) of the parameter α in which the force acting on a thick piston differs substantially from the force acting on the corresponding infinitely thin piston. For instance, in the DGDD case one can notice that when $\alpha \in [0, \pi/4]$ the force on the infinitely thin piston presents a point of stable equilibrium while for a piston of finite thickness the force always tend to move it towards the right end of the piston configuration. This appears to be a very interesting occurrence and shows that in certain circumstances the Casimir force acting on a thick piston behaves quite differently than the force on

the corresponding infinitely thin piston.

V. CONCLUDING REMARKS

In this paper we have analyzed the Casimir energy and force for thick piston configurations endowed with general boundary conditions These configurations are modeled by considering a product manifold $[0, L] \times N$ and by dividing it into three distinct regions separated by the manifolds $N_{a-\epsilon/2}$ and $N_{a+\epsilon/2}$. The thick piston itself, of thickness ϵ, is represented by the region between the cross-sections $N_{a-\epsilon/2}$ and $N_{a+\epsilon/2}$. Here we have utilized the spectral zeta function regularization technique in order to compute the Casimir energy and the corresponding force. It is important to point out that the results presented in the previous Sections are very general and are valid for any compact smooth Riemannian base manifold N and any separated boundary conditions that lead to a problem with positive eigenvalues. The explicit expressions for the Casimir energy and force obtained in Sections III and IV have been specialized in the previous Section with the purpose of illustrating a series of particular examples. For the sake of simplicity, we considered cases in which only the thickness of the piston, ϵ, and one of the parameters describing the boundary conditions, α, are allowed to vary. It is worth mentioning that due to the general nature of our results one could easily construct and analyze examples different than the ones considered here by imposing any combination of allowed boundary conditions and by using any allowed thickness ϵ.

The work performed here lends itself to a number of generalizations especially with regard to the geometry of the piston configuration. For instance it would be interesting to consider thick spherical pistons with general boundary conditions; this analysis would extend to thick pistons the results obtained in [11]. An additional straightforward generalization consists in studying thick cylindrical pistons with general boundary conditions. The calculations needed to obtain the Casimir energy and force in these cases would follow the ones presented here with the only difference arising from replacing the sine and cosine functions, obtained as solution to (2.2), with the eigenfunctions of the radial equation for the sphere or cylinder. Recently, some work has been focused on the effect that additional dimensions could have on the Casimir force, see e.g. [9, 10, 18, 26, 28]. It would be interesting to extend the results obtained here to include thick pistons with additional Kaluza-Klein dimensions. A particularly compelling analysis would be centered on trying to answer the question of how the extra dimensions affect the force on pistons of different thickness and general boundary conditions. Perhaps one could find an ideal combination of thickness and boundary conditions that would somewhat facilitate the detection of possible extra dimensions by measuring the Casimir force

on a thick piston.

---

[1] Actor A.A. and Bender I., Casimir effect for soft boundaries, *Phys. Rev.* D **52**, 3581 (1995)

[2] Barton G., Casimir piston and cylinder, perturbatively, *Phys. Rev.* D **73**, 065018 (2006)

[3] Beauregard M., Fucci G., Kirsten K., and Morales P., Casimir effect in the presence of external fields, *J. Phys. A: Math. Theor.* **46**, 115401 (2013)

[4] Blau S. K., Visser M., and Wipf A., Zeta functions and the Casimir Energy, *Nucl. Phys. B* **310**, 163 (1988)

[5] Bordag M., Klimchitskaya G. L., Mohideen U. and Mostepanenko V. M., Advances in the Casimir Effect, (Oxford University Press, Oxford) (2009)

[6] Bytsenko A. A., Cognola G., Elizalde E., Moretti V. and Zerbini S., Analytic Aspects of Quantum Fields, (World Scientific Publishing, Singapore) (2003)

[7] Casimir H. B. G., On the attraction between two perfectly conducting plates, *Proc. K. Ned. Akad. Wet. B* **51**, 793 (1948)

[8] Cavalcanti R. M., Casimir force on a piston, *Phys. Rev.* D **69**, 065015 (2004)

[9] Cheng H. The asymptotic behavior of Casimir force in the presence of compactified universal extra dimensions, *Phys. Lett.* B **643** 311, (2006)

[10] Cheng H., The Casimir force on a piston in the spacetime with extra compactified dimensions, *Phys. Lett.* B **668** 72, (2008)

[11] Dowker J. S., Spherical Casimir Pistons, *Class. Quantum Grav.* **28** 155018 (2011)

[12] Edery A., Multidimensional cut-off technique, odd-dimensional Epstein zeta functions and Casimir energy for massless scalar fields, *J. Phys. A* **39**, 685 (2006)

[13] Edery A., Casimir piston for massless scalar field in three dimensions, *Phys. Rev.* D **75**, 105012 (2007)

[14] Edery A., and Marachevsky V.N., Compact dimensions and the Casimir effect: the Proca connection, *J. High Energy Phys.* **12**, 035 (2008)

[15] Elizalde E., Odintsov S. D., Romeo A., Bytsenko A. A. and Zerbini S., Zeta Regularization Techniques with Applications, (World Scientific, Singapore) (1994)

[16] Elizalde E., Ten Physical Applications of the Spectral Zeta Function, (Springer-Verlag, Berlin) (1995)

[17] Elizalde E. and Romeo A., One-dimensional Casimir effect perturbed by an external field, *J. Phys. A: Math. Gen.* **30**, 5393 (1997)

[18] Frank M., Turan I., and Ziegler L., Casimir force in RandallSundrum models, *Phys. Rev.* D **76** 015008, (2007)

[19] Fucci G., Kirsten K., and Morales P., Pistons modeled by potentials, in *Cosmology, Quantum Vacuum, and Zeta Functions*, eds. S. Odintsov, D. Sáez-Gómez, and S. Xambó, (Springer-Verlag, Berlin, 2011) p. 313-322.

[20] Fucci G., and Kirsten K., The Casimir effect for generalized piston geometries, *Int. J. Mod. Phys. A* **27**, 1260008 (2012)

[21] Fucci G., Casimir pistons with general boundary conditions, *Nucl. Phys. B* **891**, 676 (2015)

[22] Fucci G., Graham C., and Kirsten K., Spectral functions for regular Sturm-Liouville problems, *J. Math. Phys.* **56**, 043503 (2015)

[23] Gilkey P. B., Invariance Theory the Heat Equation and the Atiyah-Singer Index Theorem, (Boca raton: CRC Press) (1995)

[24] Hertzberg M. P., Jaffe R. L., Kardar M., and Scardicchio A., Attractive Casimir forces in a closed geometry, *Phys. Rev. Lett.* **95**, 250402 (2005)

[25] Hertzberg M. P., Jaffe R. L., Kardar M., and Scardicchio A., Casimir forces in a piston geometry at zero and finite temperatures, *Phys. Rev.* D **76**, 045016 (2007)

[26] Hofmann S., Poppenhaeger K., Hossenfelder S., and Bleicher M., The Casimir effect in the presence of compactified universal extra dimensions, *Phys. Lett.* B **582** 1, (2004)

[27] Kirsten K., Spectral Functions in Mathematics and Physics, (Boca Raton: CRC Press) (2001)

[28] Kirsten K. and Fulling S. A., Kaluza-Klein models as pistons, *Phys. Rev.* D **79**, 065019 (2009)

[29] Li X.-Z., Cheng H.-B., Li J.-M., and Zhai X.-H., Attractive and repulsive nature of the Casimir force in a rectangular cavity, *Phys. Rev.* D **56**, 2155 (1997)

[30] Marachevsky V. N., Casimir interaction of two plates inside a cylinder, *Phys. Rev.* D **75**, 085019 (2007)

[31] Milton K. A., The Casimir effect: physical manifestations of zero-point energy, (World Scientific Publishing, Singapore) (2001)

[32] Milonni P. W., The Quantum Vacuum: An Introduction to Quantum Electrodynamics, (Academic Press, New York) (1994)

[33] Mostepanenko V. M. and Trunov N. N., The Casimir Effect and Its Applications, (Clarendon, Oxford) (1997)

[34] Romeo A. and Saharian A. A., Casimir effect for scalar fields under Robin boundary conditions on plates, *J. Phys. A: Math. Gen.* **35**, 1297 (2002)

[35] Teo L. P., Finite temperature Casimir effect for scalar field with Robin boundary conditions in spacetime with extra dimensions, *JHEP* **06**, 076 (2009)

[36] Teo L.P., Casimir piston of real materials and its application to multilayer models, *Phys. Rev.* A **81**, 032502 (2010)

[37] Vassilevich D. V., Heat kernel expansion: User's manual, *Phys. Rep.* **388**, 279 (2003).

[38] Zettl A., Sturm-Liouville Theory, Mathematical Surveys and Monographs Vol. 121, (American Mathematical Society) (2005)